Effects of Flow Field on Diffusion Flame Structure

T. Takeno, M. Nishioka and H. Yamashita
Department of Mechanical Engineering, Nagoya University
Chikusa-ku, Nagoya, 464-01 Japan

ABSTRACT

A laminar diffusion flame may be established in a variety of flow fields and the flame structure, comprised of a thin reaction zone and outer diffusion layers of fuel and oxidizer, may depend on the specific flow field in which the flame is established. In the present study the characteristic diffusion time of the outer diffusion layer was proposed as a linkage parameter to describe effects of the flow field on the diffusion flame structure, and a numerical study was made to test this proposal for stable flames that do not lead to local extinction. The fuel and oxidizer adopted were methane and air, respectively, and the calculation was done with detailed chemical reaction mechanisms of C2 chemistry. The flames studied were three counterflow flames and one axisymmetric coflow flame. The former are an axisymmetric counterflow flame, a rectangular counterflow flame and a tubular counterflow flame, and can be described in terms of the similarity solution, which makes the calculation into a relatively simple 1D calculation. On the other hand, the calculation of the coflow flame requires a time-consuming 2D calculation, and a newly developed 2D-Code, with an adaptive mesh adjusted for flame structure, was used. The complete elliptic partial differential equations were solved so as to account for the exact effects of a dead space formed at the leading edge of the flame. The study has revealed that there is a remarkable similarity in the structure of the diffusion flames in different flow fields with the same diffusion time. The agreement of mole production rate profiles is more excellent than those of temperature and concentration profiles. It has been shown that the diffusion time not only governs the structure of the outer diffusion layer but also controls chemical reactions proceeding inside the reaction zone, and is the most appropriate parameter to describe the effects of a flow field on the diffusion flame structure.

INTRODUCTION

What is a laminar diffusion flame? Any laminar flames in which the fuel and oxidizer are initially separated are called diffusion flames. In this definition, we may more appropriately call the flame a laminar nonpremixed flame. In the non-premixed flame, however, most of the chemical reaction occurs in a narrow reaction zone that can be approximated as a surface. The structure suggests that the combustion rate of the flame is controlled by supply rates of fuel and oxidizer to the reaction zone by molecular diffusion. This is the reason why we call the laminar nonpremixed flame a diffusion flame. The diffusion flame may be established in a variety of flow fields and the flame structure may depend on the specific flow field in which the flame is established. How can we describe this effect, and is there any chance of describing it in a universal manner ? This is the problem to be answered in this study.

The asymptotic analysis of the flame suggests that the diffusion flame structure in any flow field is comprised of a thin reaction zone and outer diffusion layers of fuel and oxidizer, surrounding the reaction zone [1]. We proposed that the characteristic diffusion time of the outer diffusion layer can be used to describe the effects of the flow field [2-4]. This is based on the following idea [3]. In the species conservation equation, the contribution of the convective term is not important in the thin reaction zone and chemical reaction is balanced by molecular diffusion. In the outer diffusion layers, on the other hand, molecular diffusion is balanced by convection. Then the local flow field can affect the flame structure only through the convection in the outer diffusion layers, and will determine concentration distributions in the diffusion layers. The concentration gradients at the boundary between the diffusion layer and the reaction zone are determined accordingly. The gradient can be used to evaluate the characteristic diffusion time of the diffusion layer. In addition, it will control what happens in the reaction zone through the supply rate of reactants to that zone. This is the reason why we can make use of the characteristic diffusion time as a linkage parameter to link diffusion flames in different flow fields.

In the present study we try to test the above proposal for stable flames that do not lead to local extinction. A numerical approach is most convenient, provided that calculations with detailed chemical reaction mechanisms can be implemented, since we can make use of numerical experiments [3] to compare the detailed flame structure in different flow fields for identical values of the diffusion time. Some similar attempts have already been made in the past [5-9] on the basis of the laminar flamelet model [10]. The scalar dissipation rate, instead of the diffusion time, was used as a linkage parameter, and the comparison of flame structure was made in the phase space of concentration vs. mixture fraction. The scalar dissipation rate is essentially the same quantity as the diffusion time, as it is just the inverse of the diffusion time. However, we believe that the concept of a diffusion time, based on the flame structure in

physical space, is much easier to understand. In addition, we believe that the physical implications of the concept have not yet fully been made clear. In diffusion flames in general, the concentration distributions in the outer diffusion layers may still depend on the local flow field even for matched values of a linkage parameter. What we can expect more generally is the similarity of reaction rates in the narrow reaction zone, being independent of the flow field, since the diffusion time determines the supply rate of reactants. In this sense, the comparison of mole production rates in the physical plane is essential [16].

NUMERICAL MODEL

The fuel and oxidizer adopted were methane and air, respectively, at atmospheric pressure. The thermochemical parameters and transport properties were calculated using CHEMKIN. Thermal diffusion was considered only for H and H2. The chemical reaction mechanism adopted was the so-called C2 chemistry, compiled by Miller and Bowman [11], including the prompt and thermal NO formation mechanisms. It involves 52 species and 235 elementary reactions. In the present study the characteristic diffusion time was defined in the following way [2]. To begin with, the apparent reaction zone position was defined as the position where the local heat release rate becomes maximum. The concentration gradient at this position was adopted to approximate that of the boundary between the reaction zone and the diffusion layer. The conserved scalar Z was defined by the normalized concentration of N2 to give values of unity and 0 for fuel and oxidizer, respectively. The local scalar dissipation rate X_q was defined by the gradient of Z normal to the reaction zone at the apparent reaction zone position by

$$X_q = D_q | \nabla Z |_q^2,$$

where D_q is the representative diffusion coefficient at the apparent reaction zone position. The characteristic diffusion time t_D is the inverse of the scalar dissipation rate and is given by

$$t_D = 1/X_q \ .$$

The flames studied were three counterflow diffusion flames and one axisymmetric coflow diffusion flame. The former are an axisymmetric counterflow flame, a rectangular counterflow flame and a tubular counterflow flame, and can be described in terms of a similarity solution, which reduces the governing equations to ordinary differential equations and makes the numerical calculation relatively simple. The numerical models of the three flames are shown schematically in Fig. 1. The temperatures of the injected methane and air were room temperature, 300 K. For the axisymmetric flame, the nozzle distance L was 1.5 cm and 3.0 cm, and the fuel and air injection velocities u_F and u_o were kept equal and were changed from 5 to 180 cm/s. Some calculations were made while keeping u_F at 16 cm/s and changing u_o from 8 to 32 cm/s. L was kept at 1.5 cm for the rectangular flame, and u_F and u_o were kept equal and changed from 5 to 60 cm/s. In the tubular flame, the fuel was injected from the inner cylinder surface and the air from the outer cylinder surface. The calculation was done for two sets of the cylinder radius: 0.5 cm inner and 2.0 cm outer, and 1.5 cm inner and 3.0 cm outer. u_F and u_o were kept equal and changed from 10 to 60 cm/s. The calculation of these flames was done in the same way as in the previous studies [12-15] by using a modified CHEMKIN 1D-Code.

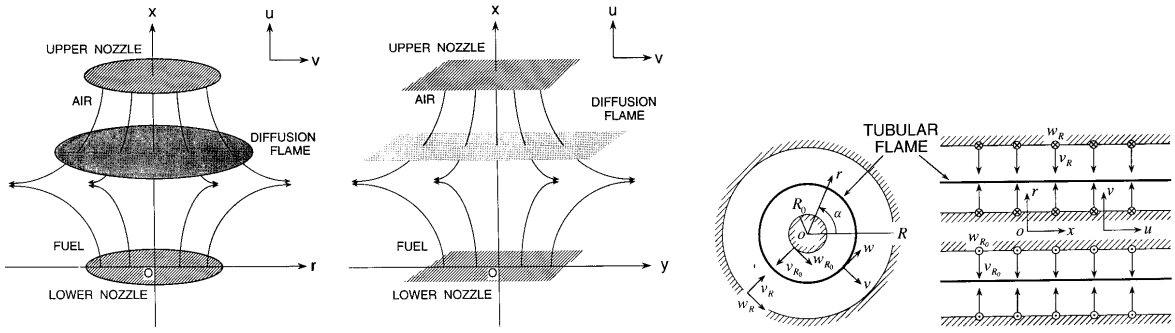

Figure 1 Numerical models of three counterflow diffusion flames; left, axisymmetric flame, center, rectangular flame, right, tubular flame.

On the other hand, the numerical model and boundary conditions of the coflow diffusion flame are shown in Fig. 2. The fuel injector radius was 0.2 cm, and the fuel at room temperature was injected in parallel to the surrounding air flow with a fully developed velocity distribution.

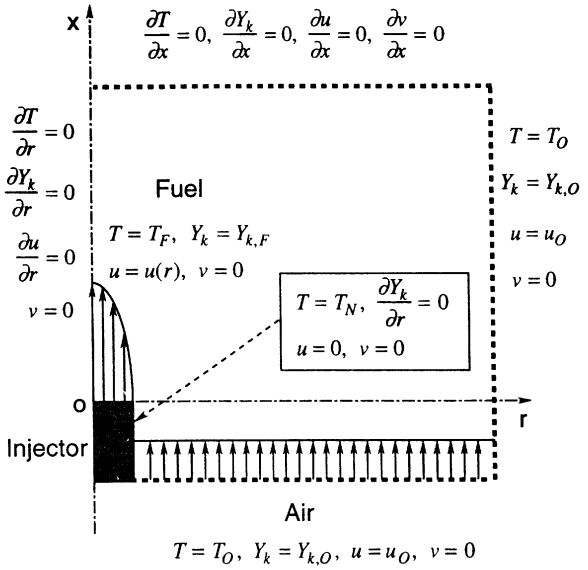

Figure 2 Numerical model and boundary conditions of axisymmetric coflowing diffusion flame.

The average injection velocity was 50 cm/s. The air at room temperature was injected at 0.5 cm upstream of the injector exit with a uniform velocity of 50 cm/s. A boundary layer develops naturally along the injector outer wall which has zero thickness. The injector wall temperature was set to 700 K, which is the value measured experimentally by the present authors. The calculation of flame structure requires a time-consuming 2D calculation, and a newly developed 2D-Code, with an adaptive mesh adjusted for flame structure, was used [16]. The complete elliptic partial differential equations were solved so as to account for the exact effects of a dead space formed at the leading edge of the flame.

RESULTS OF CALCULATION

1. COMPARISON OF THREE COUNTERFLOW FLAMES

Figure 3 shows the relation between the aerodynamic time t_a and t_D calculated for the three counterflow flames. The former was defined by $L/(u_F + u_o)$, and is just the inverse of the more familiar velocity gradient. As is seen in the figure, there exists a universal relationship between t_a and t_D common to the three counterflow flames. The relationship is independent of flame configuration, nozzle distance and fuel and air injection velocities, and gives a one-to-one correspondence between the velocity gradient and the proposed characteristic diffusion time.

Figure 4 compares the flame structure of axisymmetric flames for three combinations of L, u_F and u_o, with the same value of t_a. Profiles of temperature T and mole fraction X_i of main species are compared. The similarity of the three flame structures is remarkable, and we see that the flame structure is mostly determined by t_a, or by t_D, being independent of L, u_F and u_o. On the other hand, the calculated structure of the three types of flame changed with t_D; the flame thickness becomes larger and larger with an increase in t_D, while keeping similar temperature and concentration profiles of the main species. However, when a comparison was made of the structure of three type flame for identical values of t_D, it was found that there is a remarkable similarity in the structure, as will be seen clearly in Figs. 6-9 shown later.

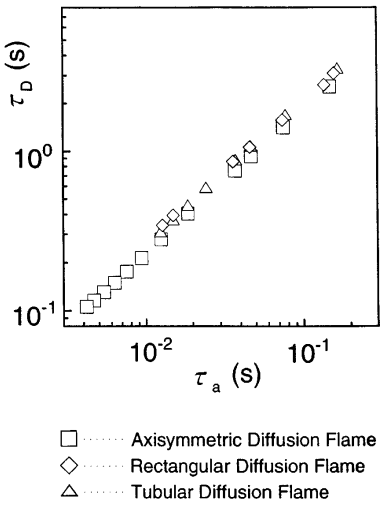

Figure 3 Correlation of aerodynamic time t_a with diffusion time t_D of three counterflow diffusion flames.

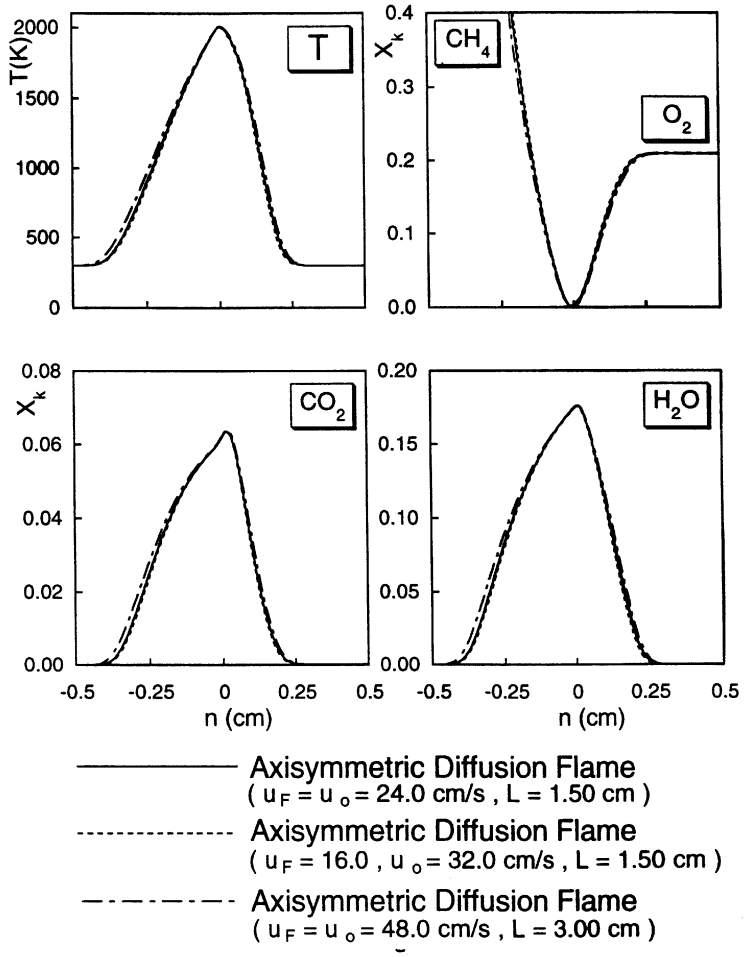

Figure 4 Comparison of flame structure of axisymmetric counterflow flame for three combinations of nozzle distance L, fuel injection velocity u_F and air injection velocity u_o, with same value of aerodynamic time t_a = 31.3 ms.

It may be said, therefore, that the structure of counterflow flames is governed by the proposed diffusion time being independent of the flame configuration, nozzle distance and fuel and air injection velocities. In view of the fact that there is a one-to-one correspondence between the diffusion time and the velocity gradient, we may use either of them to characterize the flame structure. However, the flow fields of the three counterflow flames are very similar by origin, and the above result may be regarded as just the natural consequence of this similarity. The problem is, therefore, how these counterflow flame structures correlate with that of the coflow flame.

2. COMPARISON OF COFLOW FLAME WITH COUNTERFLOW FLAMES

Figures 5a-5d show the calculated coflow diffusion flame structure [16]. Distributions of temperature, NO mole fraction, NO_2 mole fraction and NO molar production rate are shown, respectively. In the figures the apparent flame surface, defined by a locus of the peak in local heat release rate profile, is described by a solid line. Note that the *r*-axis in Fig. 5d is expanded for clearness. As is seen in Figure 5a the flame is stabilized at an upstream point near the exit along the outer wall of the injector. From this attachment point the diffusion flame develops downstream expanding in the radial direction. The characteristic features of the flame are discussed elsewhere [16] and hence the description is abbreviated here. In the following, this flame structure along the coordinate normal to the apparent flame surface is compared with those of the previous counterflow flames. The comparison was made at the three representative points along the flame surface, corresponding to t_D = 0.842 s, 1.76 s and 2.98 s, as shown in Fig. 5a.

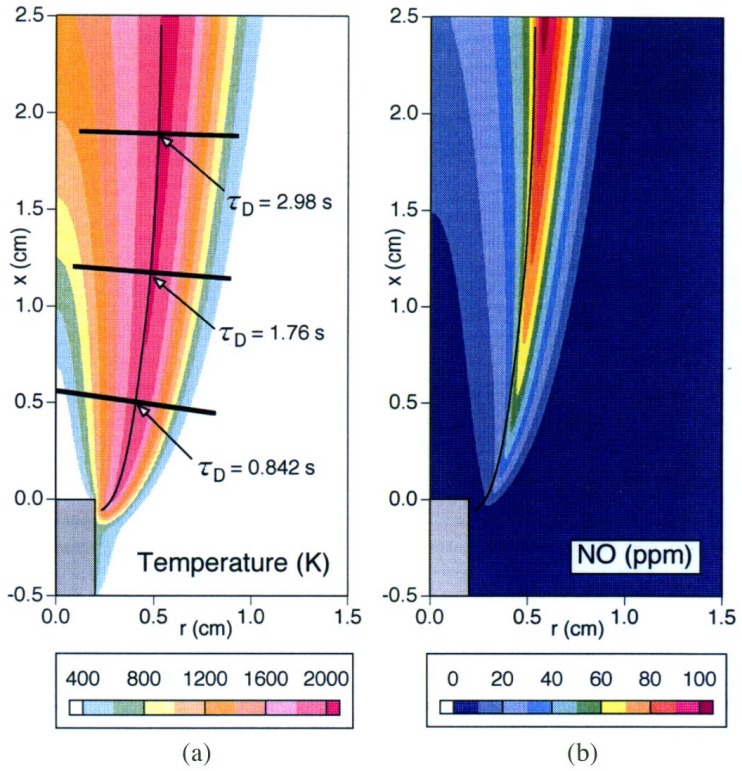

Figure 5.1 Flame structure of coflowing diffusion flame with apparent flame surface represented by solid line: distributions of (a) temperature and (b) NO.

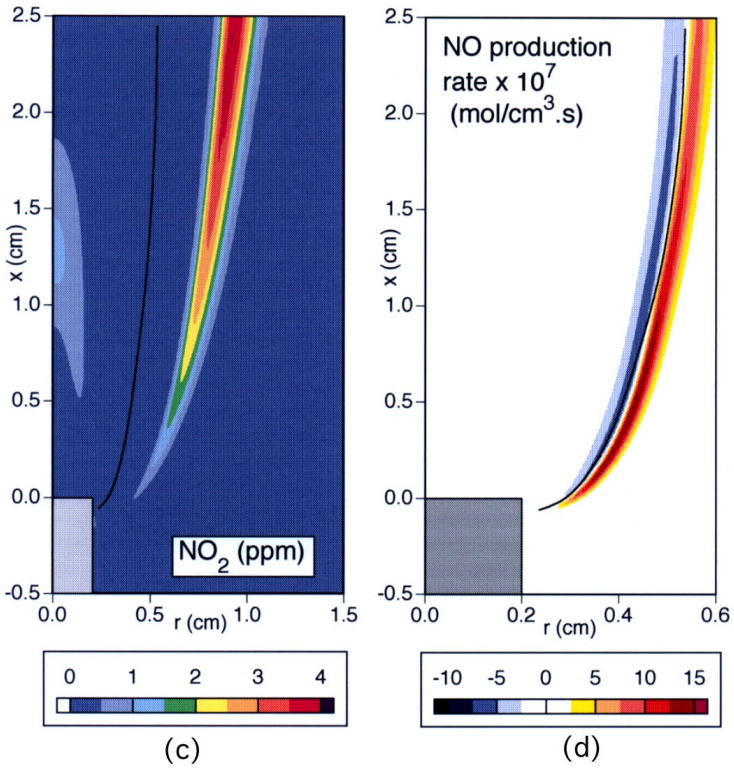

Figure 5.2 Flame structure of coflowing diffusion flame with apparent flame surface represented by solid line: distributions of (c) NO_2 concentration and (d) NO production rate.

Figures 6-9 compare the upstream flame structures at t_D = 0.842 s with those of the three counterflow flames with same value of t_D. The origin of the space coordinate n is the peak position of the heat release rate, and the solid line and the three dashed lines correspond to the coflow flame and the counterflow flames, respectively. Figure 6 shows that the temperature and the major species concentration distributions of the four flames agree remarkably well, although some slight discrepancies are observed at their skirts on the fuel side.

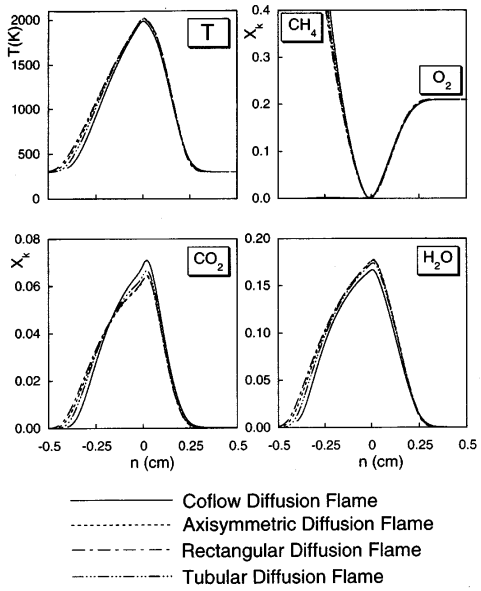

Figure 6 Comparison of flame structure of four flames with same value of diffusion time t_D = 0.842 s; profiles of temperature and mole fractions of major species.

The distributions of minor species are compared as well in Fig. 7. As is seen in the figure, the concentrations in the coflow flame are slightly lower than those in the counterflow flames, except for the CH concentration for which the agreement is perfect. The appearance of an NO2 distribution on the fuel side of the coflow flame, is the result of leakage of O2 into the fuel stream through the dead space at the leading edge [16].

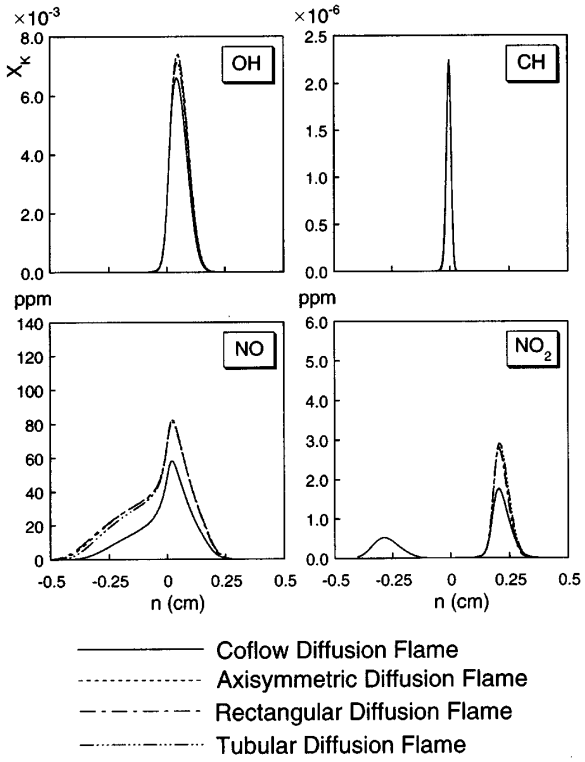

Figure 7 Comparison of flame structure of four flames with same value of diffusion time t_D = 0.842 s; profiles of mole fractions of minor species.

Figures 8 and 9 compare the mole production rate profiles of main and minor species, respectively. Although some slight discrepancies in the peak values are observed, the agreement of the profiles is almost perfect, and we notice that the agreement of the mole production rate profiles is better than that of the concentration profiles. Comparison of the middle- and down-stream flame structures with those of the counterflow flames was also made [17].

The reaction zone, as well as the outer diffusion layers, are expanded downstream, and the discrepancies in the temperature and concentration profiles increase slightly. The latter is presumably due to the fact that the contribution of the convective term becomes somewhat more important in the expanded reaction zone. However, the general trend is identical with that described above, and the agreement of the flame structure is remarkable here again. This agreement suggests that t_D is an appropriate parameter to link diffusion flames in different flow fields.

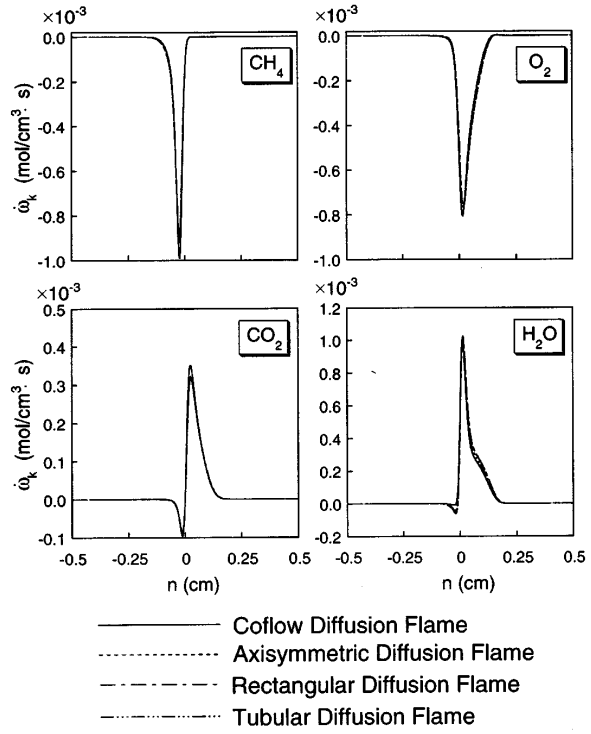

Figure 8 Comparison of flame structure of four flames with same value of diffusion time t_D = 0.842 s; profiles of mole production rate of major species.

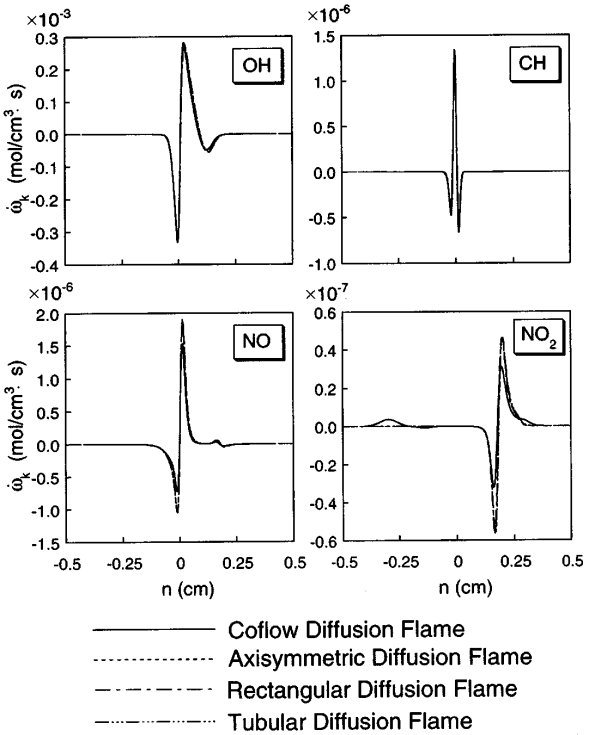

Figure 9 Comparison of flame structure of four flames with same value of diffusion time t_D = 0.842 s; profiles of mole production rate of minor species.

Figure 10 compares the distributions of flow velocity normal to the apparent flame surface for the three values of t_D. Please notice that the velocity component parallel to the surface has no effects on the flame structure. As is seen in the figure, there is a definite similarity among the distributions in the three counterflow flames, and also there is a certain similarity in the general trend of the counterflow flames and of the coflow flame. However, the discrepancy between the two types of flame is so large that it is almost impossible to introduce any common parameters, such as the velocity gradient or stretch, to correlate the flow field of the coflow flame with that of the counterflow flames. We must give up the idea of characterizing the flame structure in terms of simple flow parameters. On the other hand, the proposed diffusion time includes effects of the local flow field, in addition to those of molecular diffusion, and we believe that this is the most appropriate parameter to link the diffusion flame structures in different flow fields.

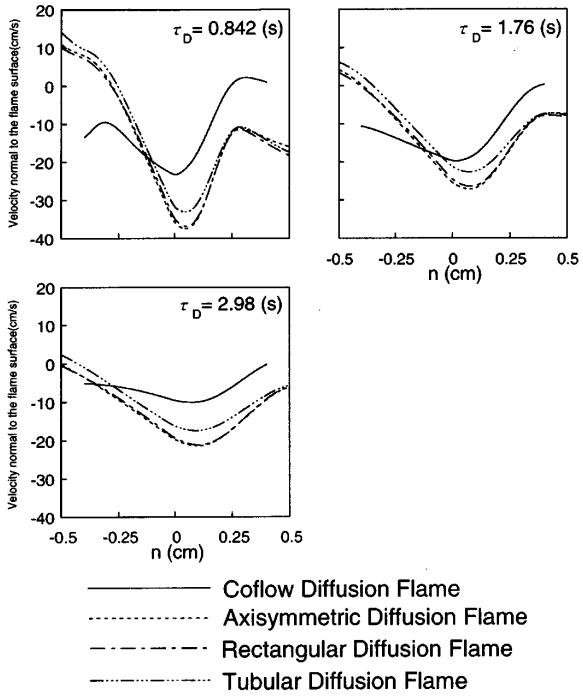

Figure 10 Comparison of the distribution of flow velocity normal to the apparent flame surface of coflow flame (solid line) and three counterflow flames (dashed lines) for three different diffusion time t_D.

3. MOLE PRODUCTION RATE AND NO EMISSION INDEX

The excellent agreement of mole production rates profiles, not only of major species but also of minor species, suggests that chemical reactions proceeding in the narrow reaction zone are actually controlled by the supply rates of reactants to the zone by molecular diffusion. This can be seen clearly in Figs. 11 and 12, in which mole production rates per unit flame surface area of major and minor species, respectively, are shown as a function of t_D for the four flames. The mole production rate is obtained by integrating mole production rate per unit volume along the space coordinate *n*. As is seen in Fig. 11, the mole production rates of major species are unique functions of τ_D, being independent of the flame type. They are inversely proportional to the square root of t_D. These species are the reactants supplied to, or the products taken away from, the reaction zone by molecular diffusion Their consumption or production rates are governed by the molecular diffusion rates in the outer diffusion layers, rather than by the reaction rates in the reaction zone. The molecular diffusion rate is directly proportional to the concentration gradient, and hence is inversely proportional to the square root of t_D by definition.

On the other hand, the minor species shown in Fig. 12 are produced and destroyed inside the reaction zone alone, and their production rates should depend in a complicated way on the chemical kinetics proceeding inside the reaction zone. However, the fair agreement between the four flames suggests that the ultimate production rate is mostly governed by the supply rate of the original reactants such as CH4 and

O2. That is, what happens inside the reaction zone is mostly governed by the supply rates of the reactants to that zone, and the local flow field affects this only through t_D. This gives further evidence that t_D is the most appropriate parameter to represent the effects of the local flow field on the diffusion flame structure. It is interesting to note that the NO production rate is rather insensitive to t_D and remains almost constant in a wide range of t_D. The combination of the production rate of NO and the consumption rate of CH4 gives the emission index of NO, that is mass production of NO per unit mass consumption of CH4. The result is shown in Fig. 13. The agreement of the four flames suggests that this curve gives a universal relationship common to all diffusion flames. We can make use of this relationship to predict the NO emission index of any type of laminar diffusion flame.

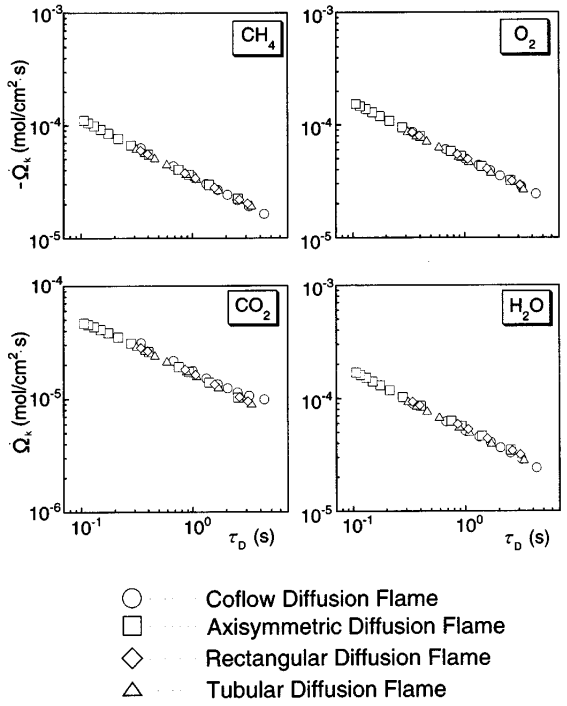

Figure 11 Mole production rates per unit flame surface area of major species as functions of characteristic diffusion time t_D for four type flames.

Although the computational domain used in this study does not cover the whole flame, and the results obtained are limited to the upstream half of the coflow diffusion flame and we have to continue further studies, the implication of the results so far obtained should be very important [16]. If we adopt an appropriate linkage parameter, such as the representative diffusion time, we can make use of the counterflow diffusion flame calculation to predict the essential characteristics of diffusion flames in other flow fields which do not lead to local extinction. Another crucial problem is the prediction of local extinction. Although the present study is concerned only with the stable flame structure, there is a chance that the proposed diffusion time can be used to predict the local extinction in general flow fields in just the same way as the critical scalar dissipation rate [10]. In general, the extinction of laminar diffusion flames has so far been discussed in terms of the velocity gradient, or the stretch rate. As is shown in Fig. 10, however, the velocity gradient is not an adequate parameter to describe effects of the local flow in general flow fields. It is more reasonable to adopt the critical diffusion time to predict the local extinction. In fact we have proposed this concept in our recent paper on the local extinction of jet diffusion flames [18].

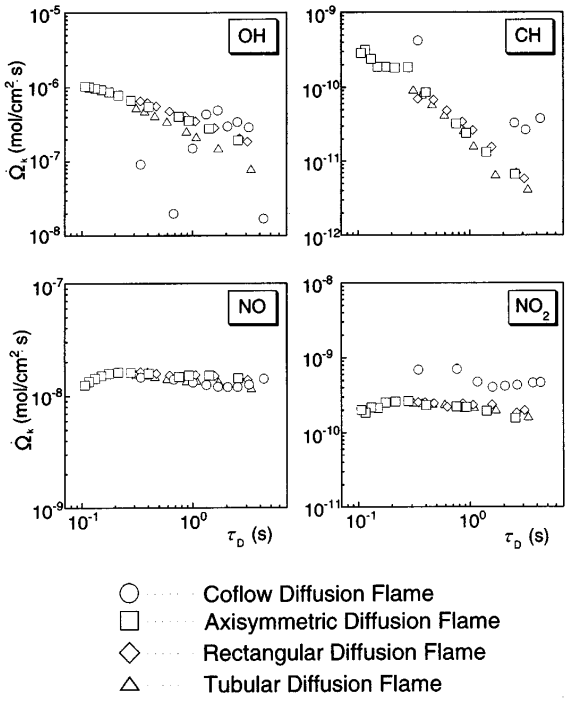

Figure 12 Mole production rates per unit flame surface area of minor species as functions of characteristic diffusion time t_D for four type flames.

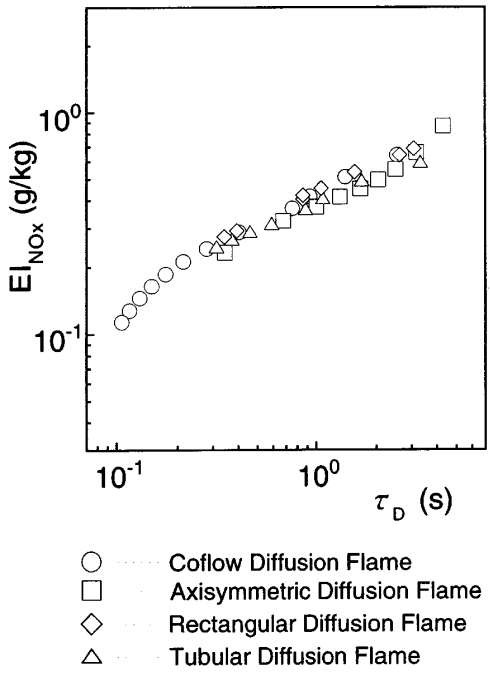

Figure 13 NO emission index of four type flames as a function of characteristic diffusion time t_D.

CONCLUDING REMARKS

In the present study the characteristic diffusion time of the outer diffusion layer was proposed as a linkage parameter to describe effects of the flow field on the diffusion flame structure, and the numerical study to test the proposal for stable flames that do not lead to local extinction has led to the following conclusions.

1. In the three types of counterflow flames there is a one-to-one correspondence between the velocity gradient and the proposed characteristic diffusion time, and we may use either of them to characterize the flame structure. However, in general flow fields we do not have such a correspondence.
2. There is a remarkable similarity in the structure of the diffusion flames in different flow fields with the same diffusion time. The agreement of mole production rate profiles is more excellent than those of temperature and concentration profiles. The diffusion time not only governs the structure of the outer diffusion layer but also controls chemical reactions proceeding inside the reaction zone, and is the most appropriate parameter to describe the effects of a flow field on the diffusion flame structure.
3. The mole consumption rates of the reactants per unit flame surface area, as well as the production rates of the main products, are controlled by the molecular diffusion rates in the outer diffusion layer, and are inversely proportional to the square root of the diffusion time.
   Furthermore, the mole production rates of the minor species, produced and destroyed inside the reaction, are mostly governed by the diffusion time. The emission index of NO is given as a unique function of the diffusion time.

ACKNOWLEDGMENT

The authors would like to extend their sincere thanks to Prof. K.N.C. Bray for his helpful discussions and special thanks to Mr. Y. Takemoto and Mr. S. Esaki for their help in this study. This work is partly supported by a Grant-in-Aid from the Ministry of Education and Culture (No.07455094).

REFERENCES

1. Williams, F. A., *Combustion Theory*, 2nd ed., The Benjamin/Cummings, Menlo Park, 1985, p. 76.
2. Takeno, T., Nishioka, M. and Yamashita, H., *Turbulence and Molecular Processes in Combustion* (T. Takeno, Ed.), Elsevier, Amsterdam, 1993, pp. 375-391.
3. Takeno, T., *Twenty-Fifth Symposium (International) on Combustion*, The Combustion Institute, Pittsburgh, 1994, pp. 1061-1073.
4. Yamashita, H., Nishioka, M., and Takeno, T., *Modeling in Combustion Science* (J. D. Buckmaster and T. Takeno, Eds.), Springer-Verlag, Heidelberg, 1995, pp. 59-67.
5. Seshadri, K., Mauss, F., Peters, N. and Warnatz, J., *Twenty-Third Symposium (International) on Combustion*, The Combustion Institute, Pittsburgh, 1990, pp. 559-560.
6. Smooke, M.D., Lin, P., Lam, J.K., and Long, M.B., *Twenty-Third Symposium (International) on Combustion*, The Combustion Institute, Pittsburgh, 1990, pp. 575-582.
7. Smooke, M. D., Xu, Y., Zurn, R. M., Lin, P., Frank, J. H. and Long, M. B., *Twenty-Fourth Symposium (International) on Combustion*, The Combustion Institute, Pittsburgh, 1992, pp. 813-821.
8. Norton, T.S., Smyth, K.C., Miller, J.H. and Smooke, M.D., *Combust. Sci. Technol.* 90:1-34 (1993).
9. Leung, K.M. and Lindsted, R.P., *Combust. Flame* 102: 129-160 (1995).
10. Peters, N., *Prog. Ener. Combust. Sci.* 10: 319-339 (1984).
11. Miller, J. A. and Bowman, C. T., *Prog. Ener. Combust. Sci.* 15: 287-338 (1989).
12. Nishioka, M., Nakagawa, S., Ishikawa, Y., and Takeno, T., *Prog. Astronaut. Aeronaut.*, Vol. 151: 141-162 (1993).
13. Takeno, T. and Nishioka, M., *Combust. Flame* 92: 465-468 (1993).
14. Nishioka, M., Nakagawa, S., Ishikawa, Y., and Takeno, T., *Combust. Flame* 98: 127-138 (1994).
15. Takeno, T., "NO Emission Characteristics and Formation Mechanisms of Methane Air Flames", *The Eighth International Symposium on Transport Phenomena in Combustion*, Tailor & Francis, in press.
16. Nishioka, M., Takemoto, Y., Yamashita, H. and Takeno, T, "Effects of Multi-dimensionality on Diffusion Flame Structure", *Twenty-Sixth Symposium (International) on Combustion*, The Combustion Institute, Pittsburgh, in press.
17. Y. Takemoto, "Prediction of NOx Emission in Diffusion Flames", Master Thesis, Graduate School, Nagoya University, March 1996.
18. Yamashita, H., Shimada, M., and Takeno, T, "A Numerical Study on Flame Stability at Transition Point of Jet Diffusion Flames", *Twenty-Sixth Symposium (International) on Combustion*, The Combustion Institute, Pittsburgh, in press.